

Bose-Einstein Correlations in $e^+e^- \rightarrow W^+W^-$ at 172 and 183 GeV

The OPAL Collaboration

Abstract

Bose-Einstein correlations between like-charge pions are studied in hadronic final states produced by e^+e^- annihilations at center-of-mass energies of 172 and 183 GeV. Three event samples are studied, each dominated by one of the processes $W^+W^- \rightarrow q\bar{q}\ell\bar{\nu}_\ell$, $W^+W^- \rightarrow q\bar{q}q\bar{q}$, or $(Z^0/\gamma)^* \rightarrow q\bar{q}$. After demonstrating the existence of Bose-Einstein correlations in W decays, an attempt is made to determine Bose-Einstein correlations for pions originating from the same W boson and from different W bosons, as well as for pions from $(Z^0/\gamma)^* \rightarrow q\bar{q}$ events. The following results are obtained for the individual chaoticity parameters λ , assuming a common source radius R:

$$\begin{aligned}\lambda^{\text{same}} &= 0.63 \pm 0.19 \pm 0.14, \\ \lambda^{\text{diff}} &= 0.22 \pm 0.53 \pm 0.14, \\ \lambda^{Z^*} &= 0.47 \pm 0.11 \pm 0.08, \\ R &= 0.92 \pm 0.09 \pm 0.09 \text{ fm.}\end{aligned}$$

In each case, the first error is statistical and the second is systematic. At the current level of statistical precision it is not established whether Bose-Einstein correlations between pions from different W bosons exist or not.

The OPAL Collaboration

G. Abbiendi², K. Ackerstaff⁸, G. Alexander²³, J. Allison¹⁶, N. Altekamp⁵, K.J. Anderson⁹, S. Anderson¹², S. Arcelli¹⁷, S. Asai²⁴, S.F. Ashby¹, D. Axen²⁹, G. Azuelos^{18,a}, A.H. Ball¹⁷, E. Barberio⁸, R.J. Barlow¹⁶, R. Bartoldus³, J.R. Batley⁵, S. Baumann³, J. Bechtluft¹⁴, T. Behnke²⁷, K.W. Bell²⁰, G. Bella²³, A. Bellerive⁹, S. Bentvelsen⁸, S. Bethke¹⁴, S. Betts¹⁵, O. Biebel¹⁴, A. Biguzzi⁵, S.D. Bird¹⁶, V. Blobel²⁷, I.J. Bloodworth¹, P. Bock¹¹, J. Böhme¹⁴, D. Bonacorsi², M. Boutemour³⁴, S. Braibant⁸, P. Bright-Thomas¹, L. Brigliadori², R.M. Brown²⁰, H.J. Burckhart⁸, P. Capiluppi², R.K. Carnegie⁶, A.A. Carter¹³, J.R. Carter⁵, C.Y. Chang¹⁷, D.G. Charlton^{1,b}, D. Chrisman⁴, C. Ciocca², P.E.L. Clarke¹⁵, E. Clay¹⁵, I. Cohen²³, J.E. Conboy¹⁵, O.C. Cooke⁸, C. Couyoumtzelis¹³, R.L. Coxe⁹, M. Cuffiani², S. Dado²², G.M. Dallavalle², R. Davis³⁰, S. De Jong¹², A. de Roeck⁸, P. Dervan¹⁵, K. Desch⁸, B. Dienes^{33,d}, M.S. Dixit⁷, J. Dubbert³⁴, E. Duchovni²⁶, G. Duckeck³⁴, I.P. Duerdoth¹⁶, D. Eatough¹⁶, P.G. Estabrooks⁶, E. Etzion²³, F. Fabbri², M. Fanti², A.A. Faust³⁰, F. Fiedler²⁷, M. Fierro², I. Fleck⁸, R. Folman²⁶, A. Fürtjes⁸, D.I. Futyan¹⁶, P. Gagnon⁷, J.W. Gary⁴, J. Gascon¹⁸, S.M. Gascon-Shotkin¹⁷, G. Gaycken²⁷, C. Geich-Gimbel³, G. Giacomelli², P. Giacomelli², V. Gibson⁵, W.R. Gibson¹³, D.M. Gingrich^{30,a}, D. Glenzinski⁹, J. Goldberg²², W. Gorn⁴, C. Grandi², K. Graham²⁸, E. Gross²⁶, J. Grunhaus²³, M. Gruwé²⁷, G.G. Hanson¹², M. Hansroul⁸, M. Hapke¹³, K. Harder²⁷, A. Harel²², C.K. Hargrove⁷, C. Hartmann³, M. Hauschild⁸, C.M. Hawkes¹, R. Hawkings²⁷, R.J. Hemingway⁶, M. Herndon¹⁷, G. Herten¹⁰, R.D. Heuer²⁷, M.D. Hildreth⁸, J.C. Hill⁵, P.R. Hobson²⁵, M. Hoch¹⁸, A. Hocker⁹, K. Hoffman⁸, R.J. Homer¹, A.K. Honma^{28,a}, D. Horváth^{32,c}, K.R. Hossain³⁰, R. Howard²⁹, P. Hüntemeyer²⁷, P. Igo-Kemenes¹¹, D.C. Imrie²⁵, K. Ishii²⁴, F.R. Jacob²⁰, A. Jawahery¹⁷, H. Jeremie¹⁸, M. Jimack¹, C.R. Jones⁵, P. Jovanovic¹, T.R. Junk⁶, D. Karlen⁶, V. Kartvelishvili¹⁶, K. Kawagoe²⁴, T. Kawamoto²⁴, P.I. Kayal³⁰, R.K. Keeler²⁸, R.G. Kellogg¹⁷, B.W. Kennedy²⁰, D.H. Kim¹⁹, A. Klier²⁶, S. Kluth⁸, T. Kobayashi²⁴, M. Kobel^{3,e}, D.S. Koetke⁶, T.P. Kokott³, M. Kolrep¹⁰, S. Komamiya²⁴, R.V. Kowalewski²⁸, T. Kress⁴, P. Krieger⁶, J. von Krogh¹¹, T. Kuhl³, P. Kyberd¹³, G.D. Lafferty¹⁶, H. Landsman²², D. Lanske¹⁴, J. Lauber¹⁵, S.R. Lautenschlager³¹, I. Lawson²⁸, J.G. Layter⁴, D. Lazic²², A.M. Lee³¹, D. Lellouch²⁶, J. Letts¹², L. Levinson²⁶, R. Liebisch¹¹, B. List⁸, C. Littlewood⁵, A.W. Lloyd¹, S.L. Lloyd¹³, F.K. Loebinger¹⁶, G.D. Long²⁸, M.J. Losty⁷, J. Ludwig¹⁰, D. Liu¹², A. Macchiolo², A. Macpherson³⁰, W. Mader³, M. Mannelli⁸, S. Marcellini², C. Markopoulos¹³, A.J. Martin¹³, J.P. Martin¹⁸, G. Martinez¹⁷, T. Mashimo²⁴, P. Mättig²⁶, W.J. McDonald³⁰, J. McKenna²⁹, E.A. Mckigney¹⁵, T.J. McMahon¹, R.A. McPherson²⁸, F. Meijers⁸, S. Menke³, F.S. Merritt⁹, H. Mes⁷, J. Meyer²⁷, A. Michelini², S. Mihara²⁴, G. Mikenberg²⁶, D.J. Miller¹⁵, R. Mir²⁶, W. Mohr¹⁰, A. Montanari², T. Mori²⁴, K. Nagai⁸, I. Nakamura²⁴, H.A. Neal¹², B. Nellen³, R. Nisius⁸, S.W. O’Neale¹, F.G. Oakham⁷, F. Odoricci², H.O. Ogren¹², M.J. Oreglia⁹, S. Orito²⁴, J. Pálinkás^{33,d}, G. Pásztor³², J.R. Pater¹⁶, G.N. Patrick²⁰, J. Patt¹⁰, R. Perez-Ochoa⁸, S. Petzold²⁷, P. Pfeifenschneider¹⁴, J.E. Pilcher⁹, J. Pinfold³⁰, D.E. Plane⁸, P. Poffenberger²⁸, J. Polok⁸, M. Przybycien⁸, C. Rembser⁸, H. Rick⁸, S. Robertson²⁸, S.A. Robins²², N. Rodning³⁰, J.M. Roney²⁸, K. Roscoe¹⁶, A.M. Rossi², Y. Rozen²², K. Runge¹⁰, O. Runolfsson⁸, D.R. Rust¹², K. Sachs¹⁰, T. Saeki²⁴, O. Sahr³⁴, W.M. Sang²⁵, E.K.G. Sarkisyan²³, C. Sbarra²⁹, A.D. Schaile³⁴, O. Schaile³⁴, F. Scharf³, P. Scharff-Hansen⁸, J. Schieck¹¹, B. Schmitt⁸, S. Schmitt¹¹, A. Schöning⁸, M. Schröder⁸, M. Schumacher³, C. Schwick⁸, W.G. Scott²⁰,

R. Seuster¹⁴, T.G. Shears⁸, B.C. Shen⁴, C.H. Shepherd-Themistocleous⁸, P. Sherwood¹⁵,
G.P. Siroti², A. Sittler²⁷, A. Skuja¹⁷, A.M. Smith⁸, G.A. Snow¹⁷, R. Sobie²⁸,
S. Söldner-Rembold¹⁰, S. Spagnolo²⁰, M. Sproston²⁰, A. Stahl³, K. Stephens¹⁶,
J. Steuerer²⁷, K. Stoll¹⁰, D. Strom¹⁹, R. Ströhmer³⁴, B. Surov⁸, S.D. Talbot¹, S. Tanaka²⁴,
P. Taras¹⁸, S. Tarem²², R. Teuscher⁸, M. Thiergen¹⁰, J. Thomas¹⁵, M.A. Thomson⁸, E. von
Törne³, E. Torrence⁸, S. Towers⁶, I. Trigger¹⁸, Z. Trócsányi³³, E. Tsur²³, A.S. Turcot⁹,
M.F. Turner-Watson¹, I. Ueda²⁴, R. Van Kooten¹², P. Vannerem¹⁰, M. Verzocchi¹⁰,
H. Voss³, F. Wäckerle¹⁰, A. Wagner²⁷, C.P. Ward⁵, D.R. Ward⁵, P.M. Watkins¹,
A.T. Watson¹, N.K. Watson¹, P.S. Wells⁸, N. Wermes³, J.S. White⁶, G.W. Wilson¹⁶,
J.A. Wilson¹, T.R. Wyatt¹⁶, S. Yamashita²⁴, G. Yekutieli²⁶, V. Zacek¹⁸, D. Zer-Zion⁸

¹School of Physics and Astronomy, University of Birmingham, Birmingham B15 2TT, UK

²Dipartimento di Fisica dell' Università di Bologna and INFN, I-40126 Bologna, Italy

³Physikalisches Institut, Universität Bonn, D-53115 Bonn, Germany

⁴Department of Physics, University of California, Riverside CA 92521, USA

⁵Cavendish Laboratory, Cambridge CB3 0HE, UK

⁶Ottawa-Carleton Institute for Physics, Department of Physics, Carleton University, Ottawa, Ontario K1S 5B6, Canada

⁷Centre for Research in Particle Physics, Carleton University, Ottawa, Ontario K1S 5B6, Canada

⁸CERN, European Organisation for Particle Physics, CH-1211 Geneva 23, Switzerland

⁹Enrico Fermi Institute and Department of Physics, University of Chicago, Chicago IL 60637, USA

¹⁰Fakultät für Physik, Albert Ludwigs Universität, D-79104 Freiburg, Germany

¹¹Physikalisches Institut, Universität Heidelberg, D-69120 Heidelberg, Germany

¹²Indiana University, Department of Physics, Swain Hall West 117, Bloomington IN 47405, USA

¹³Queen Mary and Westfield College, University of London, London E1 4NS, UK

¹⁴Technische Hochschule Aachen, III Physikalisches Institut, Sommerfeldstrasse 26-28, D-52056 Aachen, Germany

¹⁵University College London, London WC1E 6BT, UK

¹⁶Department of Physics, Schuster Laboratory, The University, Manchester M13 9PL, UK

¹⁷Department of Physics, University of Maryland, College Park, MD 20742, USA

¹⁸Laboratoire de Physique Nucléaire, Université de Montréal, Montréal, Quebec H3C 3J7, Canada

¹⁹University of Oregon, Department of Physics, Eugene OR 97403, USA

²⁰CLRC Rutherford Appleton Laboratory, Chilton, Didcot, Oxfordshire OX11 0QX, UK

²²Department of Physics, Technion-Israel Institute of Technology, Haifa 32000, Israel

²³Department of Physics and Astronomy, Tel Aviv University, Tel Aviv 69978, Israel

²⁴International Centre for Elementary Particle Physics and Department of Physics, University of Tokyo, Tokyo 113-0033, and Kobe University, Kobe 657-8501, Japan

²⁵Institute of Physical and Environmental Sciences, Brunel University, Uxbridge, Middlesex UB8 3PH, UK

²⁶Particle Physics Department, Weizmann Institute of Science, Rehovot 76100, Israel

²⁷Universität Hamburg/DESY, II Institut für Experimental Physik, Notkestrasse 85, D-22607 Hamburg, Germany

²⁸University of Victoria, Department of Physics, P O Box 3055, Victoria BC V8W 3P6,

Canada

²⁹University of British Columbia, Department of Physics, Vancouver BC V6T 1Z1, Canada

³⁰University of Alberta, Department of Physics, Edmonton AB T6G 2J1, Canada

³¹Duke University, Dept of Physics, Durham, NC 27708-0305, USA

³²Research Institute for Particle and Nuclear Physics, H-1525 Budapest, P O Box 49, Hungary

³³Institute of Nuclear Research, H-4001 Debrecen, P O Box 51, Hungary

³⁴Ludwigs-Maximilians-Universität München, Sektion Physik, Am Coulombwall 1, D-85748 Garching, Germany

^a and at TRIUMF, Vancouver, Canada V6T 2A3

^b and Royal Society University Research Fellow

^c and Institute of Nuclear Research, Debrecen, Hungary

^d and Department of Experimental Physics, Lajos Kossuth University, Debrecen, Hungary

^e on leave of absence from the University of Freiburg

1 Introduction

In reactions leading to hadronic final states Bose-Einstein correlations (BEC) between identical bosons are well known. These correlations lead to an enhancement of the number of identical bosons over that of non-identical bosons when the two particles are close to each other in phase space. Experimentally this effect was first observed for pions by Goldhaber et al. [1]. For recent reviews see, for example, reference [2]. In e^+e^- annihilations at center-of-mass energies of 91 GeV, BEC have been observed for charged pion pairs [3–6], for $K_S^0 K_S^0$ pairs [7–10] and also for $K^\pm K^\pm$ [11].

In the present paper we report on an investigation of BEC for charged pions between e^+e^- reactions at center-of-mass energies of 172 and 183 GeV, above the threshold for W -pair production. The analysis is motivated by the question of whether BEC for pions from different W bosons exist or not. Theoretically this question is still not settled [12, 13]. However, if such correlations do exist, this could bias significantly the measurement of the W boson mass in fully hadronic W -pair events [12, 14–16]. The DELPHI collaboration has published a measurement, at $\sqrt{s} = 172$ GeV, of BEC between pions originating from two different W bosons [17], in which basically BEC in $W^+W^- \rightarrow q\bar{q}\ell\bar{\nu}_\ell$ events were subtracted from those of $W^+W^- \rightarrow q\bar{q}q\bar{q}$ events. The aim of the present analysis is to analyse BEC for fully hadronic W -pair events ($W^+W^- \rightarrow q\bar{q}q\bar{q}$), semileptonic W -pair events ($W^+W^- \rightarrow q\bar{q}\ell\bar{\nu}_\ell$), as well as non-radiative $(Z^0/\gamma)^* \rightarrow q\bar{q}$ events. After having established BEC in hadronic W decays, BEC are investigated separately for three classes of pions: those originating from the same W boson, those from different W bosons and those from non-radiative $(Z^0/\gamma)^* \rightarrow q\bar{q}$ events. Note that in this analysis, tracks are not assigned to jets or W -bosons and no kinematic fits are needed.

BEC between identical bosons can be formally expressed in terms of the normalised

function

$$C(Q) = \frac{\rho_2(p_1, p_2)}{\rho_1(p_1)\rho_1(p_2)} = \sigma \frac{d^2\sigma}{dp_1 dp_2} / \left\{ \frac{d\sigma}{dp_1} \frac{d\sigma}{dp_2} \right\}, \quad (1)$$

where σ is the total boson production cross section, $\rho_1(p_i)$ and $d\sigma/dp_i$ are the single-boson density in momentum space and the inclusive cross section, respectively. Similarly $\rho_2(p_1, p_2)$ and $d^2\sigma/dp_1 dp_2$ are respectively the density of the two-boson system and its inclusive cross section. The product of the independent one-particle densities $\rho_1(p_1)\rho_1(p_2)$ is referred to as the reference density distribution, to which the measured two-particle distribution is compared. The inclusive two-boson density $\rho_2(p_1, p_2)$ can be written as:

$$\rho_2(p_1, p_2) = \rho_1(p_1)\rho_1(p_2) + K_2(p_1, p_2), \quad (2)$$

where $K_2(p_1, p_2)$ represents the two-body correlations. In the simple case of two identical bosons the normalised density function $C(Q)$, defined in Eq. 1, describes the two-body correlations. Thus one has

$$C(Q) = 1 + \tilde{K}_2(p_1, p_2), \quad (3)$$

where $\tilde{K}_2(p_1, p_2) = K_2(p_1, p_2)/[\rho_1(p_1)\rho_1(p_2)]$ is the normalised two-body correlation term. Since BEC are present when the bosons are close to one another in phase space, a natural choice is to study them as a function of the Lorentz invariant variable Q defined by

$$Q^2 = -(p_1 - p_2)^2 = M_2^2 - 4\mu^2,$$

which approaches zero as the identical bosons move closer in phase space. Here p_i is the four-momentum vector of the i th particle, μ is the boson mass (here m_π) and M_2^2 is the invariant mass squared of the two-boson system. Ideally the reference sample should contain all correlations present in the sample used to measure $\rho(p_1, p_2)$, other than the BEC, such as those due to energy, momentum and charge conservation, resonance decays and global event properties. In this analysis, the reference is chosen to be a sample of unlike-charge pairs of pions from the same event. Since the presence of the resonances ω , K_S^0 , η , η' , ρ^0 , f_0 and f_2 in the unlike-charge reference sample leads to kinematic correlations which are not present in the like-charge sample, the unlike-charge sample has to be corrected for this effect using simulated events.

Assuming a spherically symmetric pion source with a Gaussian radial distribution, the correlation function $C(Q)$ can be parametrised [1] by

$$C(Q) = N (1 + f_\pi(Q) \lambda e^{-Q^2 R^2}) (1 + \delta Q + \epsilon Q^2), \quad (4)$$

where R is the radius of the source and λ represents the strength of the correlation, with $0 \leq \lambda \leq 1$. A value of $\lambda = 1$ corresponds to a fully chaotic source, while $\lambda = 0$ corresponds to a completely coherent source without any BEC. The function $f_\pi(Q)$ is the probability that a selected track pair is really a pair of pions, as a function of Q . The additional empirical term $(1 + \delta Q + \epsilon Q^2)$ takes into account the behaviour of the correlation function at high Q values due to long-range particle correlations (e.g. charge and energy conservation, phase-space constraints), and N is a normalisation factor.

The structure of the paper is as follows. Section 2 contains a brief overview of the OPAL detector, the event and track selections as well as Monte Carlo models. In section 3 the analysis of the data is described. BEC are investigated for $(Z^0/\gamma)^* \rightarrow q\bar{q}$, $W^+W^- \rightarrow$

$q\bar{q}\ell\bar{\nu}_\ell$ and $W^+W^- \rightarrow q\bar{q}q\bar{q}$ events. After establishing BEC in hadronic W-events the chaoticity parameter for BEC between the decay products from the same W, λ^{same} , and from different W bosons, λ^{diff} , are determined. Finally, section 4 summarises the results obtained.

2 Experimental Details

2.1 The OPAL detector

A detailed description of the OPAL detector has been presented elsewhere [18] and therefore only the features relevant to this analysis are summarised here. Charged particle trajectories are reconstructed using the cylindrical central tracking detectors which consist of a silicon microvertex detector, a high-precision gas vertex detector, a large-volume gas jet chamber and thin z -chambers¹. The entire central detector is contained within a solenoid that provides an axial magnetic field of 0.435 T. The silicon microvertex detector consists of two layers of silicon strip detectors, allowing to measure at least one hit per charged track in the angular region $|\cos\theta| < 0.93$. It is surrounded by the vertex drift chamber, followed by the jet chamber, about 400 cm in length and 185 cm in radius, that provides up to 159 space points per track and also measures the ionisation energy loss of charged particles, dE/dx . With at least 130 charge samples along a track, a resolution of 3.8% is achieved for the dE/dx for minimum ionising pions in jets [19, 20]. The z -chambers, which considerably improve the measurement of charged tracks in θ , follow the jet chamber at large radius. The combination of these chambers leads to a momentum resolution of $\sigma_p/p^2 = 1.25 \times 10^{-3} (\text{GeV}/c)^{-1}$. Track finding is nearly 100% efficient within the angular region $|\cos\theta| < 0.92$. The mass resolution for $K_S^0 \rightarrow \pi^+\pi^-$, related to the resolution in the correlation variable Q , is found to be $\sigma = 7.0 \pm 0.1 \text{ MeV}/c^2$ [7].

2.2 Data selection

This study is carried out using data at e^+e^- center-of-mass energies of 172 GeV and 183 GeV with integrated luminosities of approximately 10 pb^{-1} and 57 pb^{-1} , respectively. Three mutually exclusive event samples are selected: a) *the fully hadronic event sample*, $W^+W^- \rightarrow q\bar{q}q\bar{q}$, where both W bosons decay hadronically; b) *the semileptonic event sample*, $W^+W^- \rightarrow q\bar{q}\ell\bar{\nu}_\ell$, where one W decays hadronically and the other decays semileptonically; and c) hadronic non-W events $(Z^0/\gamma)^* \rightarrow q\bar{q}$, referred to here as the *the non-radiative $(Z^0/\gamma)^*$ event sample* in this analysis. Throughout this paper, a reference to W^+ or its decay products implicitly includes the charge conjugate states.

¹The OPAL right-handed coordinate system is defined such that the origin is at the geometric centre of the jet chamber, z is parallel to, and has positive sense along, the e^- beam direction, r is the coordinate normal to z , θ is the polar angle with respect to $+z$ and ϕ is the azimuthal angle around z .

2.2.1 Selection of the fully hadronic event sample $W^+W^- \rightarrow q\bar{q}q\bar{q}$

The selection of fully hadronic $W^+W^- \rightarrow q\bar{q}q\bar{q}$ events is performed in two stages using a preselection based on cuts followed by a likelihood-based selection procedure. Fully hadronic decays, $W^+W^- \rightarrow q\bar{q}q\bar{q}$ are characterised by four or more energetic hadronic jets and little missing energy. A preselection using kinematic variables removes background predominantly from radiative $(Z^0/\gamma)^* \rightarrow q\bar{q}$ events. Events satisfying the preselection criteria are subjected to a likelihood selection, which discriminates between signal and the remaining four-jet-like QCD background.

At 172 GeV, several variables based on the characteristic four-jet-like nature, momentum balance and jet angular structure, are used to distinguish $W^+W^- \rightarrow q\bar{q}q\bar{q}$ events from the remaining background and to construct the likelihood. The details of the selection at 172 GeV are described in appendix B of [21]. The signal and background situation at 183 GeV is similar to the one at 172 GeV. For this reason, no new selection strategy was developed and the event selection at 183 GeV is just a reoptimised version of the selection at 172 GeV. The details of the selection at 183 GeV are described in [22]. At 183 GeV, no cut was applied against Z^0Z^0 events.

Overall, there is a background of 11.6% from $(Z^0/\gamma)^* \rightarrow q\bar{q}$ events and a contribution of 2.1% from $e^+e^- \rightarrow Z^0Z^0 \rightarrow q\bar{q}q\bar{q}$ events. No selection for $W^+W^- \rightarrow q\bar{q}q\bar{q}$ events is applied to events selected as $W^+W^- \rightarrow q\bar{q}\ell\bar{\nu}_\ell$ events.

2.2.2 Selection of the semileptonic event sample $W^+W^- \rightarrow q\bar{q}\ell\bar{\nu}_\ell$

$W^+W^- \rightarrow q\bar{q}e\bar{\nu}_e$ and $W^+W^- \rightarrow q\bar{q}\mu\bar{\nu}_\mu$ events are characterised by two well-separated hadronic jets, a high-momentum lepton and missing momentum due to the unobserved neutrino. In $W^+W^- \rightarrow q\bar{q}\tau\bar{\nu}_\tau$ the τ lepton gives rise to a low-multiplicity jet consisting of one or three tracks. The tracks from τ decay are not used in the BEC studies. Cuts are applied to reduce the background from radiative $(Z^0/\gamma)^* \rightarrow q\bar{q}$ events. A likelihood is formed using kinematic variables and characteristics of the lepton candidate to further suppress the background from $(Z^0/\gamma)^* \rightarrow q\bar{q}$ events. The details of the selection at 172 GeV are given in appendix A of [21].

The $W^+W^- \rightarrow q\bar{q}\ell\bar{\nu}_\ell$ event selection for the 183 GeV data is a modified version of the 172 GeV selection. At 183 GeV, a looser set of preselection cuts is used since the lepton energy spectrum is broader due to the increased boost and the set of variables used in the likelihood selections is modified. In the $W^+W^- \rightarrow q\bar{q}\tau\bar{\nu}_\tau$ sample there is a significant background from hadronic decays of single W events ($e^+e^- \rightarrow W e\bar{\nu}_e$) and an additional likelihood selection is used to reduce this background. This is only applied to $W^+W^- \rightarrow q\bar{q}\tau\bar{\nu}_\tau$ events where the tau is identified as decaying in the single prong hadronic channel. Finally, in order to reduce Z^0Z^0 contribution, events passing the $W^+W^- \rightarrow q\bar{q}e\bar{\nu}_e$ likelihood selection are rejected if there is evidence of a second energetic electron. A similar procedure is applied to the $W^+W^- \rightarrow q\bar{q}\mu\bar{\nu}_\mu$ selection. The details of the selection at 183 GeV are given in [22]. There is a background of 3.5% from $(Z^0/\gamma)^* \rightarrow q\bar{q}$ events, 1.0% from $W^+W^- \rightarrow q\bar{q}q\bar{q}$ events, 1.3% from single W events and 0.8% from $Z^0Z^0 \rightarrow q\bar{q}\ell\bar{\ell}$ events.

2.2.3 Selection of the non-radiative event sample $(Z^0/\gamma)^* \rightarrow q\bar{q}$

Here, an extension of the selection criteria defined in [24] is used, which starts by selecting hadronic events defined as in [25]. To reject background from $e^+e^- \rightarrow \tau^+\tau^-$ and $\gamma\gamma \rightarrow q\bar{q}$ and to ensure that the events are well contained in the OPAL detector one requires that the event has at least seven charged tracks with transverse momentum $p_t > 150$ MeV/ c and that the polar angle of the thrust axis lies within the range $|\cos\theta_T| < 0.9$. To reject events with large initial-state radiation, one requires $\sqrt{s} - \sqrt{s'} < 10$ GeV, where $\sqrt{s'}$ is the effective invariant mass of the hadronic system [23]. For the suppression of the W^+W^- background one requires that the events are selected neither for the semileptonic nor for the fully hadronic W^+W^- samples described above. The cut in the relative likelihood for vetoing $W^+W^- \rightarrow q\bar{q}q\bar{q}$ events is looser than in the $W^+W^- \rightarrow q\bar{q}q\bar{q}$ event selection. After selection, there is a residual background of 3.8% from W -pair events and a contribution of 0.3% from Z^0Z^0 events.

2.2.4 Pion selection and Event samples

Note that the three event selections result in completely independent event samples without any overlap. After the event selection the following cuts are applied to all tracks, for all three event samples. A track is required to have a transverse momentum $p_t > 0.15$ GeV/ c , momentum $p < 10$ GeV/ c and a corresponding error of $\sigma_p < 0.1$ GeV/ c . Only tracks with polar angles θ satisfying $|\cos\theta| < 0.94$ are considered. The probability for a track to be a pion is enhanced by requiring that the pion probability P_π from the dE/dx measurement is $P_\pi > 0.02$. Pion-pairs from a K_S^0 decay are rejected using the K_S^0 finder described in [8]. This algorithm rejects 31% of the unlike-charge pion pairs coming from a K_S^0 decay. Since less than 11% of the rejected pairs do not originate from a K_S^0 , this cut does not introduce a significant bias in the Q -distribution. Finally, events with fewer than five charged selected tracks are rejected. The number of events retained, as well as the number of background events evaluated from Monte Carlo simulation is given in table 1, for all three event samples.

event sample	number of selected events		expected background events	
	172 GeV	183 GeV	172 GeV	183 GeV
$W^+W^- \rightarrow q\bar{q}q\bar{q}$	55	327	9.5 ± 0.5	43.6 ± 2.4
$W^+W^- \rightarrow q\bar{q}\ell\bar{\nu}_\ell$	45	326	2.1 ± 0.5	23.1 ± 2.4
$(Z^0/\gamma)^*$	214	1009	8.1 ± 1.7	43.2 ± 4.9

Table 1: Number of retained events and number of background events predicted for the three event samples, separately for 172 GeV and 183 GeV.

2.3 Monte Carlo models

A number of Monte Carlo models are used to model $(Z^0/\gamma)^* \rightarrow q\bar{q}$, $W^+W^- \rightarrow q\bar{q}\ell\bar{\nu}_\ell$ or $W^+W^- \rightarrow q\bar{q}q\bar{q}$ events. For the $W^+W^- \rightarrow q\bar{q}q\bar{q}$ event sample the simulated events are also used to determine the fraction of track pairs coming from the same or different W

bosons. The Monte Carlo samples are generated at e^+e^- center-of-mass energies of 172 and 183 GeV in proportion to the corresponding integrated luminosities. The production of W-pairs is simulated using KORALW [26]. Non-radiative decays $(Z^0/\gamma)^* \rightarrow q\bar{q}$ as well as the Z^0Z^0 and $We\bar{\nu}_e$ events are simulated with PYTHIA [27]. KORALW uses the same string model as PYTHIA for hadronisation. For systematic error studies the event generator HERWIG [28], which employs a cluster hadronisation model, is also used. All these Monte Carlo samples discussed above are generated without BEC. In addition W-pair events are also simulated with BEC included [16], using PYTHIA². The algorithm introduces BEC via a shift of final-state momenta among identical bosons. For these events two samples are generated: In the first, BEC are simulated for all pions in the event, both from the same and from different W bosons. In the second sample, BEC are simulated only for pions originating from the same W boson.

3 Analysis

Using the tracks that pass the selection of section 2.2.4, the Q -distributions are determined for like-charge pairs as well as for unlike-charge pairs. The correlation function $C(Q)$ is then obtained as the ratio of these Q -distributions. Coulomb interactions between charged particles affect like- and unlike-charge pairs in opposite ways and modify the correlation function. We therefore apply the following correction to the correlation function,

$$C_{\text{corr}}(Q) = \chi(Q) C_{\text{uncorr}}(Q), \quad (5)$$

where

$$\chi(Q) = \frac{e^{2\pi\eta} - 1}{1 - e^{-2\pi\eta}}, \quad (6)$$

and where $\eta = \alpha m_\pi/Q$ with α the fine-structure constant and m_π the mass of the charged pion [29]. The Coulomb correction factor $\chi(Q)$ is about 17% in the first Q bin, 5% in the second bin and 1% in the tenth bin, with a bin size of 0.08 GeV/ c^2 (see Fig. 1 for the definition of the bins). The Monte Carlo simulations do not contain Coulomb effects, so the Monte Carlo distributions are not corrected by Eq. 5.

Structure in the unlike-charge samples due to resonance production is corrected using Monte Carlo. For this, the Q -distribution is obtained for unlike-charge pair combinations taken exclusively from the decay products of K_S^0 mesons and the resonances ω , η , η' , ρ^0 , f_0 and f_2 as produced in the Monte Carlo. The production of resonances has only been measured at e^+e^- center-of-mass energies around the Z^0 peak and not at energies above the Z^0 peak. JETSET [30] describes the production of resonances around the Z^0 peak quite well, although not perfectly in all cases [31]. To estimate the contribution for each resonance to the Q -distribution at LEP 2 energies, the Q -distribution for each resonance is multiplied by the ratio of the measured production rate at LEP [31] and the corresponding rate in JETSET. The main contributions come from K_S^0 , ω , ρ^0 and η mesons. The Q -distribution for the resonances, thus obtained, is then scaled to the

²The model parameters controlling BEC in PYTHIA are taken to be MSTJ(51)=2, MSTJ(54)=-1, MSTJ(57)=1, PARJ(92)=1.0, PARJ(93)=0.4, MSTJ(52)=9, PARJ(94)=0.275, and PARJ(95)=0.0, as suggested by the authors of [16].

number of selected events and subtracted from the experimental unlike-charge reference Q -distribution. These corrections are made for each event selection separately. They are typically 5–10% for small Q , falling rapidly for $Q > 0.8 \text{ GeV}/c^2$. The three unlike-charge distributions, before the correction, and the expected signal from resonance decays are shown in Fig. 1.

The resulting experimental correlations $C(Q)$ are shown, for the three event samples separately, in Fig. 2. The data in all three distributions exhibit a clear enhancement at low Q , consistent with the presence of BEC.

3.1 Fit to establish BEC in W-pair events

The measured distributions cannot be directly compared with the parametrisation of Eq. 4 since, in general, each distribution has contributions from several physical processes that may have different BEC. To illustrate the situation, consider the hadronic W-pair events. They have as their main contribution (see Table 1) the correlations from pions coming from hadronic W decays. They contain, however, also contributions from background events, i.e. $(Z^0/\gamma)^* \rightarrow q\bar{q}$ events. Thus

$$C^{\text{had}}(Q) = \frac{N_{\pm\pm}^{\text{WW}} + N_{\pm\pm}^{Z^*}}{N_{+-}^{\text{WW}} + N_{+-}^{Z^*}}, \quad (7)$$

where $N_{\pm\pm}^{\text{WW}}$ and $N_{\pm\pm}^{Z^*}$ are the numbers of like-charge track pairs for the class of pions from $W^+W^- \rightarrow q\bar{q}q\bar{q}$ events and for the class of pions from the background sample of $(Z^0/\gamma)^* \rightarrow q\bar{q}$ events. The variables N_{+-}^{WW} and $N_{+-}^{Z^*}$ are defined analogously for unlike-charge pairs. Eq. 7 can be rewritten as

$$C^{\text{had}}(Q) = P_{\text{had}}^{\text{WW}}(Q) C^{q\bar{q}q\bar{q}}(Q) + (1 - P_{\text{had}}^{\text{WW}}(Q)) C_{\text{had}}^{Z^*}(Q), \quad (8)$$

where $C^{q\bar{q}q\bar{q}}(Q)$ and $C_{\text{had}}^{Z^*}(Q)$ are the BEC for the class of pions from $W^+W^- \rightarrow q\bar{q}q\bar{q}$ events and for the class of pions from the sample of $(Z^0/\gamma)^* \rightarrow q\bar{q}$ events, the main background in the hadronic selection. $P_{\text{had}}^{\text{WW}}(Q) = N_{+-}^{\text{WW}}/(N_{+-}^{\text{WW}} + N_{+-}^{Z^*})$ is the fraction of unlike-charge pion pairs at a given Q which originate from a W-pair event in the hadronic event sample. Here and in the following, the small number of Z^0Z^0 events are not counted as background but as signal, since their properties with regard to BEC should be quite similar.

The experimentally determined correlations for the other two event samples can be written as:

$$C^{\text{semi}}(Q) = P_{\text{semi}}^{\text{W}}(Q) C^{q\bar{q}}(Q) + (1 - P_{\text{semi}}^{\text{W}}(Q)) C^{Z^*}(Q), \quad (9)$$

for the $W^+W^- \rightarrow q\bar{q}\ell\bar{\nu}_\ell$ event sample and

$$C^{\text{non-rad.}}(Q) = P_{\text{non-rad.}}^{Z^*}(Q) C^{Z^*}(Q) + (1 - P_{\text{non-rad.}}^{Z^*}(Q)) C^{q\bar{q}q\bar{q}}(Q) \quad (10)$$

for the non-radiative $(Z^0/\gamma)^*$ event sample. The notation in these equations is analogous to that of Eq. 7. $C^{\text{semi}}(Q)$ and $C^{Z^*}(Q)$ are the BEC for the two pion classes from $W^+W^- \rightarrow q\bar{q}\ell\bar{\nu}_\ell$ and non-radiative $(Z^0/\gamma)^* \rightarrow q\bar{q}$ events, respectively. The definition of

OPAL

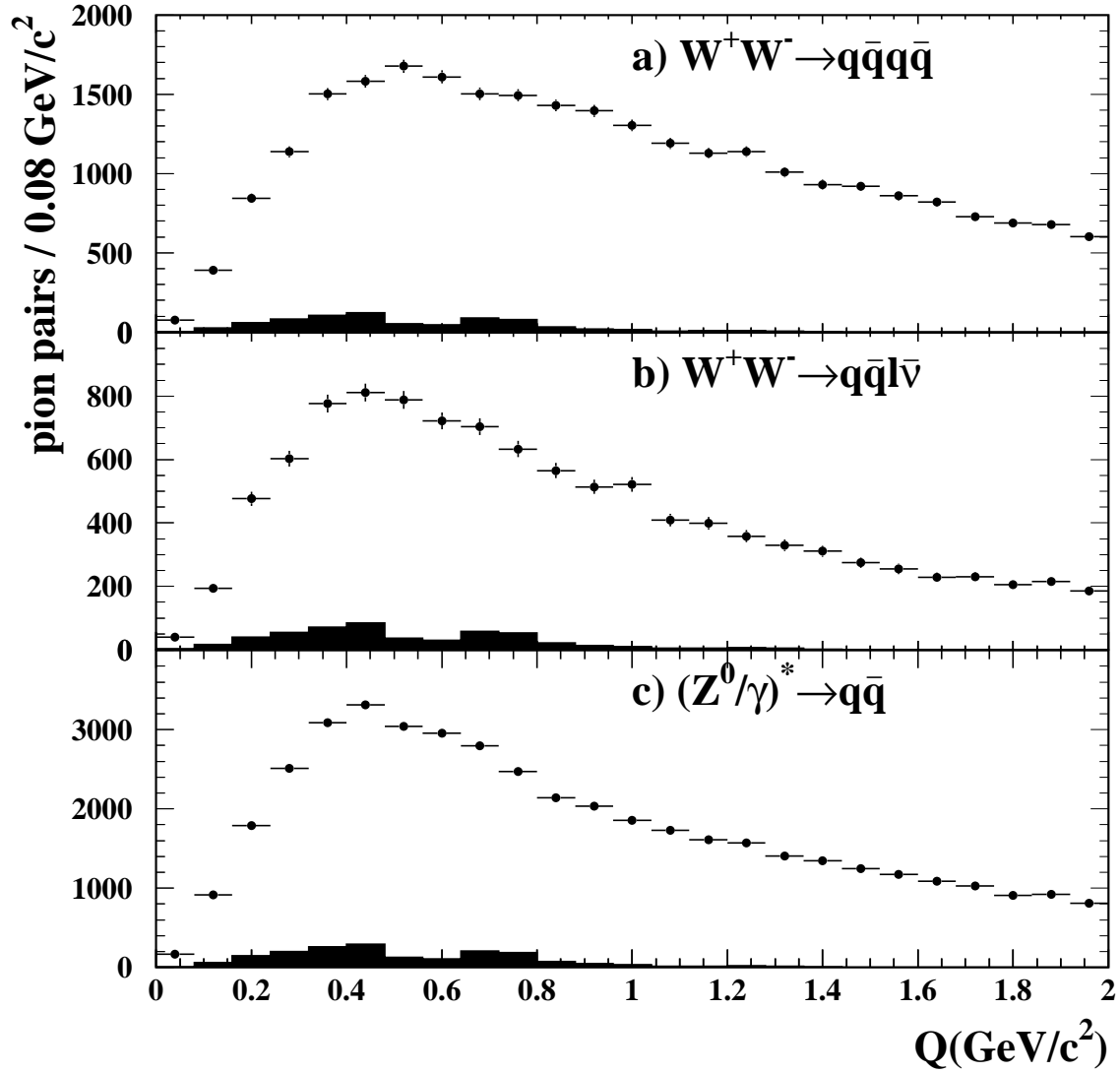


Figure 1: The points show the unlike-charge pion pair distribution, before the correction for resonance production, for the three different event selections; a) for the fully hadronic, b) for the semileptonic, and c) for the non-radiative event selection. The filled histogram is the expected contribution from resonances, where both tracks of a pion pair come from the same resonance.

OPAL

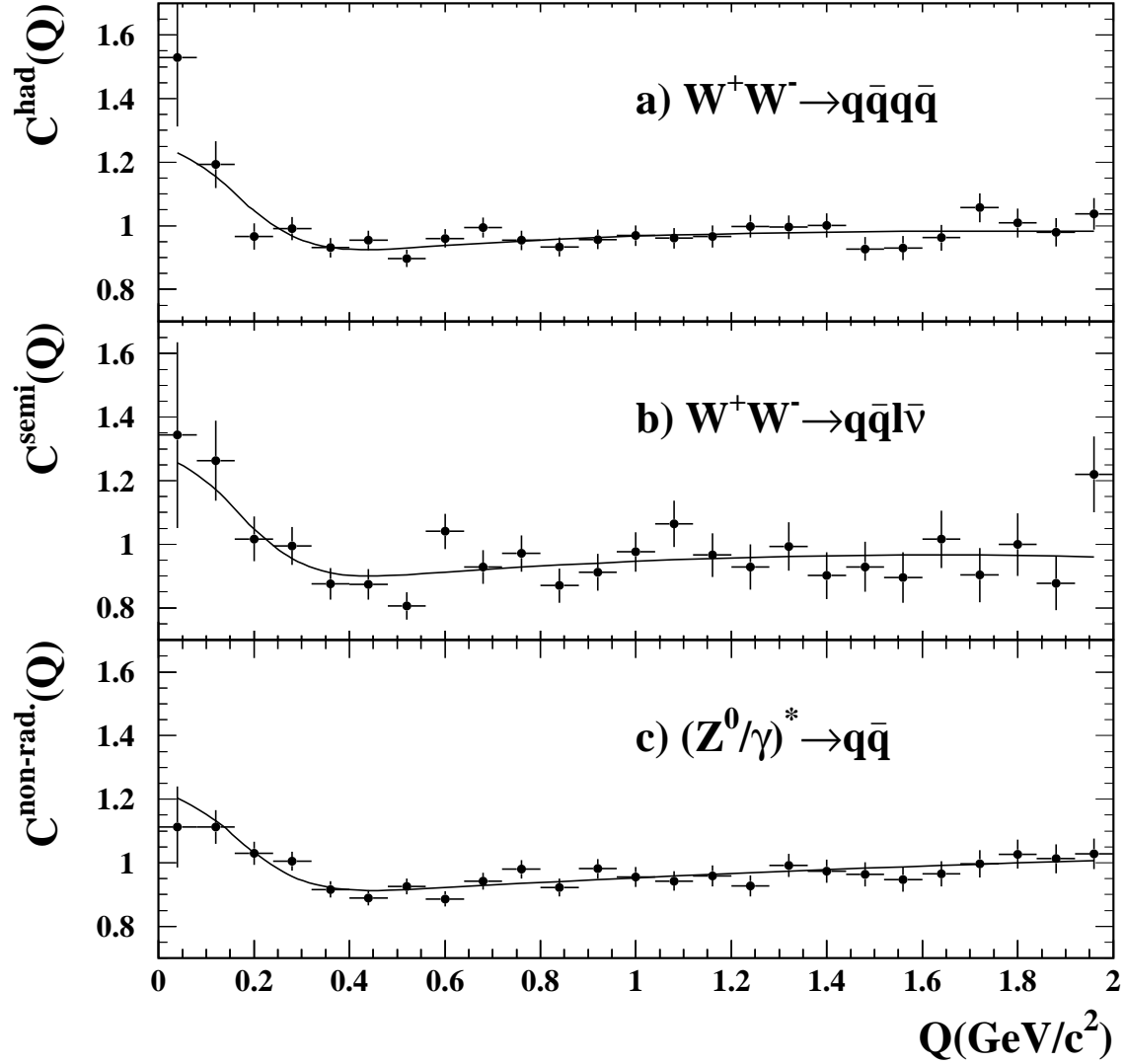


Figure 2: The correlation function for like-charge pairs relative to unlike-charge pairs for three event selections; a) $C^{\text{had}}(Q)$ for the fully hadronic, b) $C^{\text{semi}}(Q)$ for the semileptonic, and c) $C^{\text{non-rad.}}(Q)$ for the non-radiative event selection. The Coulomb-corrected data are shown as solid points together with statistical errors. The curves are the result of the simultaneous fit discussed in Sect. 3.2.

the relative fractions $P_{\text{had}}^{\text{WW}}(Q)$, $P_{\text{semi}}^{\text{W}}(Q)$ and $P_{\text{non-rad}}^{\text{Z}^*}(Q)$ is given in table 2. They are taken from a Monte Carlo simulation which does not contain BEC as discussed in section 2.3. These probabilities are global properties of the events and depend little on whether BEC are assumed or not. The small number of single-W events in the semileptonic event sample are treated as signal events.

The hadronic W-pair sample contains a sizeable number of $(Z^0/\gamma)^*$ background events. Due to the selection cuts suppressing $(Z^0/\gamma)^*$ events in the hadronic W-pair sample, the remaining $(Z^0/\gamma)^*$ events have different event shapes and multiplicities from those in the main non-radiative $(Z^0/\gamma)^*$ event sample. Since BEC depend on event shape and multiplicity [4], the correlation function for $(Z^0/\gamma)^*$ events selected as hadronic W-pairs, $C_{\text{had}}^{\text{Z}^*}(Q)$, is expected to be different from that for the main non-radiative selection, $C^{\text{Z}^*}(Q)$. To take these differences into account, the parameters λ and R in the correlation functions $C_{\text{had}}^{\text{Z}^*}(Q)$ and $C^{\text{Z}^*}(Q)$ are not taken to be equal but those in $C_{\text{had}}^{\text{Z}^*}(Q)$ are adjusted according to the different event topology. In order to estimate this correction, the $W^+W^- \rightarrow q\bar{q}q\bar{q}$ selection described in 2.2, which contains no direct center-of-mass energy dependent variables, is applied to data taken at LEP. A simultaneous BEC fit is applied to both events selected as $W^+W^- \rightarrow q\bar{q}q\bar{q}$ events and events which are not selected as $W^+W^- \rightarrow q\bar{q}q\bar{q}$ events. The differences obtained in λ and R are used here ³ to take differences in the correlation function $C_{\text{had}}^{\text{Z}^*}(Q)$ and $C^{\text{Z}^*}(Q)$ into account. Due to high purity of the semileptonic and non-radiative $(Z^0/\gamma)^*$ selections, no adjustment is applied to the correlation functions of events selected as background in $C^{\text{semi}}(Q)$ and $C^{\text{non-rad.}}(Q)$. For $W^+W^- \rightarrow q\bar{q}q\bar{q}$ events selected as fully hadronic events and $W^+W^- \rightarrow q\bar{q}q\bar{q}$ events selected as non-radiative $(Z^0/\gamma)^*$ events the same BEC are assumed. The effect of this assumption will be described with the systematic errors.

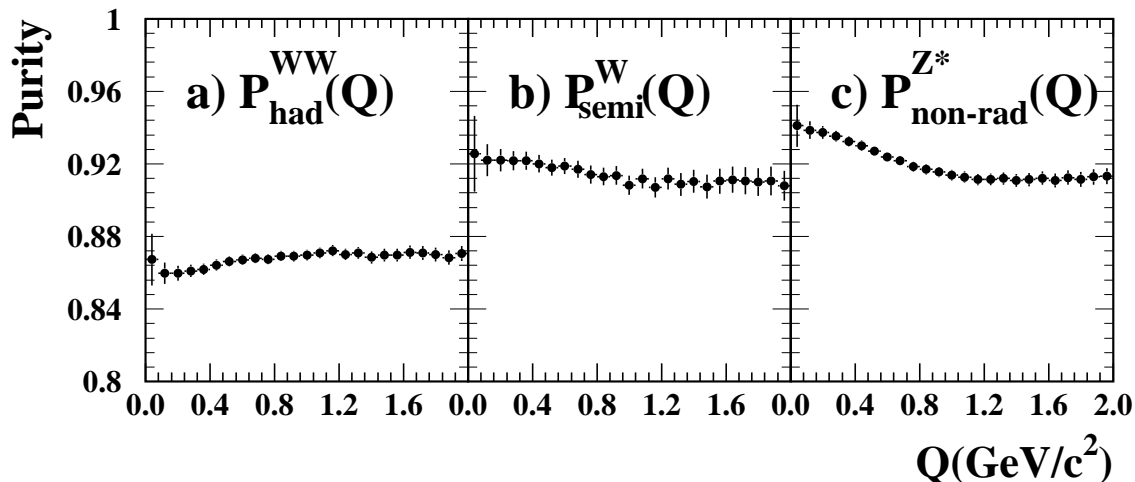


Figure 3: The purities a) $P_{\text{had}}^{\text{WW}}(Q)$, b) $P_{\text{semi}}^{\text{W}}(Q)$ and c) $P_{\text{non-rad}}^{\text{WW}}(Q)$ as obtained from Monte Carlo simulations.

³ For the function $C_{\text{had}}^{\text{Z}^*}(Q)$ the absolute λ value is reduced by 0.094 and the absolute R value is increased by 0.097 fm relative to the corresponding parameters of $C^{\text{Z}^*}(Q)$, with λ^{Z^*} kept as a free parameter in the main BEC fit.

Probability definition	Prob. that $+-$ track pair
$P_{\text{had}}^{\text{WW}}(Q) = \frac{N_{+-}^{\text{WW}}(Q)}{N_{+-}^{\text{WW}}(Q) + N_{+-}^{\text{Z}^*}(Q)}$	originates from $W^+W^- \rightarrow q\bar{q}q\bar{q}$ process, in the hadronic event selection.
$P_{\text{had}}^{\text{Z}^*}(Q) = 1 - P_{\text{had}}^{\text{WW}}(Q)$	originates from $(Z^0/\gamma)^* \rightarrow q\bar{q}$ process, in the hadronic event selection.
$P_{\text{semi}}^{\text{W}}(Q) = \frac{N_{+-}^{\text{W}}(Q)}{N_{+-}^{\text{W}}(Q) + N_{+-}^{\text{Z}^*}(Q)}$	originates from $W^+W^- \rightarrow q\bar{q}\ell\bar{\nu}_\ell$ process, in the semileptonic event selection.
$P_{\text{non-rad}}^{\text{Z}^*}(Q) = \frac{N_{+-}^{\text{Z}^*}(Q)}{N_{+-}^{\text{WW}}(Q) + N_{+-}^{\text{Z}^*}(Q)}$	originates from $(Z^0/\gamma)^* \rightarrow q\bar{q}$ process, in the non-radiative event selection.
$P_{\text{non-rad}}^{\text{WW}}(Q) = 1 - P_{\text{non-rad}}^{\text{Z}^*}(Q)$	originates from $W^+W^- \rightarrow q\bar{q}q\bar{q}$ process, in the non-radiative event selection.
$P_{\text{had}}^{\text{same}}(Q) = \frac{N_{+-}^{\text{same W}}(Q)}{N_{+-}^{\text{same W}}(Q) + N_{+-}^{\text{diff W}}(Q) + N_{+-}^{\text{Z}^*}(Q)}$	originates from the same W, in the hadronic event selection.
$P_{\text{non-rad}}^{\text{same}}(Q) = \frac{N_{+-}^{\text{same W}}(Q)}{N_{+-}^{\text{same W}}(Q) + N_{+-}^{\text{diff W}}(Q) + N_{+-}^{\text{Z}^*}(Q)}$	originates from the same W, in the non-radiative event selection.

Table 2: Definition and meaning of the various probabilities concerning unlike-charge track pairs, used in Eqs. 8 - 10 and 12 - 14 and illustrated in Figs. 3 and 4.

The unknown correlation functions $C^{q\bar{q}q\bar{q}}(Q)$, $C^{q\bar{q}}(Q)$ and $C^{Z^*}(Q)$ are parametrised using Eq. 4. The parameters are determined in a simultaneous fit to the three experimental distributions shown in Fig. 3.2. A common source radius R is used for all event classes, while the parameter λ is allowed to be different. There is justified by the typical separation between the W^+ and W^- decay vertices is smaller than 0.1 fm at LEP 2 energies, much smaller than the typical hadronic source radius of $R \approx 1$ fm [12], justifying equal source radii for the $W^+W^- \rightarrow q\bar{q}q\bar{q}$ and the $W^+W^- \rightarrow q\bar{q}\ell\bar{\nu}_\ell$ event classes. The source radius for e^+e^- annihilations into hadrons has been measured up to 90 GeV and no evidence has been found for an energy dependence [2]. For this reason R is assumed to be the same at higher energies and the same source radius is also used for the $(Z^0/\gamma)^* \rightarrow q\bar{q}$ event class. Separate fits to the distributions show also consistent radii for the different event selections. The pion probability $f_\pi(Q)$ is taken from Monte Carlo. At small values of Q it is about constant ~ 0.84 and varies only weakly with Q for all channels. The long-range parameters are expected to be different for the $W^+W^- \rightarrow q\bar{q}q\bar{q}$, $W^+W^- \rightarrow q\bar{q}\ell\bar{\nu}_\ell$ and $(Z^0/\gamma)^* \rightarrow q\bar{q}$ event class, due to kinematic and topological differences. The results for the thirteen free parameters in the fit are given in Table 3. The fit is made in the full range of $0.0 < Q < 2.0$ GeV/ c^2 . In the distributions of Fig. 2 the same particles contribute many times, in different bins of Q , which introduces bin-to-bin correlations. These are taken into account in the fit. All three experimental distributions are well described by the fit, the $\chi^2/\text{d.o.f.}$ is 76.1/62.

Parameter	$W^+W^- \rightarrow q\bar{q}q\bar{q}$	$W^+W^- \rightarrow q\bar{q}\ell\bar{\nu}_\ell$	$(Z^0/\gamma)^*$
R (fm)		$0.91 \pm 0.11 \pm 0.10$	
λ	$0.43 \pm 0.15 \pm 0.09$	$0.75 \pm 0.26 \pm 0.18$	$0.49 \pm 0.11 \pm 0.08$
N	$0.86 \pm 0.04 \pm 0.04$	$0.79 \pm 0.08 \pm 0.08$	$0.86 \pm 0.05 \pm 0.04$
δ	$0.12 \pm 0.10 \pm 0.10$	$0.29 \pm 0.23 \pm 0.24$	$0.13 \pm 0.11 \pm 0.08$
ϵ	$-0.04 \pm 0.05 \pm 0.06$	$-0.09 \pm 0.10 \pm 0.11$	$-0.02 \pm 0.05 \pm 0.04$

Table 3: Result of the simultaneous fit. The first error corresponds to the statistical uncertainty the second to systematics.

3.2 Fit to establish BEC in same and different W bosons.

In this section BEC are investigated separately for pions originating from the same W boson and for pions from different W bosons. The correlations for the fully hadronic event sample (Eq. 7) are written as

$$C^{\text{had}}(Q) = \frac{N_{\pm\pm}^{\text{same W}} + N_{\pm\pm}^{\text{diff W}} + N_{\pm\pm}^{Z^*}}{N_{+-}^{\text{same W}} + N_{+-}^{\text{diff W}} + N_{+-}^{Z^*}}, \quad (11)$$

where $N_{\pm\pm}^{\text{same W}}$, $N_{\pm\pm}^{\text{diff W}}$ and $N_{\pm\pm}^{Z^*}$ are the number of like-charge track pairs for the class of pions from the same W boson, different W bosons and from $(Z^0/\gamma)^* \rightarrow q\bar{q}$ events. The variables $N_{+-}^{\text{same W}}$, $N_{+-}^{\text{diff W}}$ and $N_{+-}^{Z^*}$ are defined, in a similar way, for unlike-charge pairs. Eq. 11 can be rewritten as

$$C^{\text{had}}(Q) = P_{\text{had}}^{\text{same}}(Q) C^{\text{same}}(Q) + P_{\text{had}}^{Z^*}(Q) C_{\text{had}}^{Z^*}(Q) + (1 - P_{\text{had}}^{\text{same}}(Q) - P_{\text{had}}^{Z^*}(Q)) C^{\text{diff}}(Q), \quad (12)$$

where $C^{\text{same}}(Q)$, $C^{\text{diff}}(Q)$ and $C^{Z^*}(Q)$ are the BEC for the class of pions from the same W boson, different W bosons and from $(Z^0/\gamma)^* \rightarrow q\bar{q}$ events. The variables $P_{\text{had}}^{\text{same}}(Q)$ and $P_{\text{had}}^{Z^*}(Q)$ are defined in Table 2. Likewise, the experimentally determined correlations for the other two event samples can be written as:

$$C^{\text{semi}}(Q) = P_{\text{semi}}^{\text{W}}(Q) C^{\text{same}}(Q) + (1 - P_{\text{semi}}^{\text{W}}(Q)) C^{Z^*}(Q) \quad (13)$$

for the $W^+W^- \rightarrow q\bar{q}\ell\bar{\nu}_\ell$ event sample and

$$C^{\text{non-rad.}}(Q) = P_{\text{non-rad}}^{\text{same}}(Q) C^{\text{same}}(Q) + P_{\text{non-rad}}^{Z^*}(Q) C^{Z^*}(Q) \\ + (1 - P_{\text{non-rad}}^{\text{same}}(Q) - P_{\text{non-rad}}^{Z^*}(Q)) C^{\text{diff}}(Q) \quad (14)$$

for the non-radiative Z^* event sample. The definition of the variables $P_{\text{had}}^{\text{same}}(Q)$, $P_{\text{had}}^{Z^*}(Q)$, $P_{\text{semi}}^{\text{W}}(Q)$, $P_{\text{non-rad}}^{\text{same}}(Q)$, and $P_{\text{non-rad}}^{Z^*}(Q)$ is also given in table 2.

By simultaneously fitting Eq's. 12, 13, and 14 to the experimental distributions in Fig. 2, the BEC for the three pion classes $C^{\text{same}}(Q)$, $C^{\text{diff}}(Q)$ and $C^{Z^*}(Q)$ are determined. Again, the probabilities $P_{\text{non-rad}}^{\text{same}}(Q)$, $P_{\text{non-rad}}^{Z^*}(Q)$, $P_{\text{had}}^{\text{same}}(Q)$, $P_{\text{had}}^{Z^*}(Q)$ and $P_{\text{semi}}^{\text{W}}(Q)$ are taken from Monte Carlo simulations not containing BEC, as discussed in section 2.3.

The functions $P_{\text{non-rad}}^{\text{same}}(Q)$ and $P_{\text{had}}^{\text{same}}(Q)$ are shown in Fig. 4. Their properties contain only information from unlike-charge pion pairs and are therefore independent of BEC. The effect of possible variations of the function $P_{\text{had}}^{\text{same}}(Q)$, if BEC are assumed in the Monte Carlo, is discussed in section 3.3. The unknown correlation functions $C^{\text{same}}(Q)$, $C^{\text{diff}}(Q)$ and $C^{Z^*}(Q)$ are parametrised using Eq. 4 with different λ for the three event classes. As before a common source radius R is used for all event classes. For the correlation function $C_{\text{had}}^{Z^*}(Q)$ the parameters λ and R are adjusted like in section 3.1. Based on Monte Carlo studies the long range parameters δ^{diff} and ϵ^{diff} for the correlation function $C^{\text{diff}}(Q)$ are taken to be zero. This is equivalent to the assumption that colour reconnection effects do not influence the Q distributions. The free fit parameters are then determined in a simultaneous fit to the three experimental distributions shown in Fig. 2. The results for the eleven free parameters in the fit are given in Table 4. The fit is made in the full range of $0.0 < Q < 2.0 \text{ GeV}/c^2$. The fit result is given in Fig. 2. All three experimental distributions are well described by the fit ($\chi^2/\text{d.o.f.}$ is 76.4/64). The correlation between the parameters λ^{diff} and λ^{same} , with a coefficient of -0.52 , is shown in Fig. 5.

Parameter	same W	diff W	$(Z^0/\gamma)^*$
R (fm)		$0.92 \pm 0.09 \pm 0.09$	
λ	$0.63 \pm 0.19 \pm 0.14$	$0.22 \pm 0.53 \pm 0.14$	$0.47 \pm 0.11 \pm 0.08$
N	$0.83 \pm 0.05 \pm 0.07$	$1.00 \pm 0.01 \pm 0.00$	$0.87 \pm 0.04 \pm 0.04$
δ	$0.21 \pm 0.15 \pm 0.19$	zero assumed	$0.11 \pm 0.11 \pm 0.07$
ϵ	$-0.07 \pm 0.07 \pm 0.08$	zero assumed	$-0.01 \pm 0.05 \pm 0.02$

Table 4: Result of the simultaneous fit distinguishing pions from the same and different W boson. The first error corresponds to the statistical uncertainty, the second one to systematics.

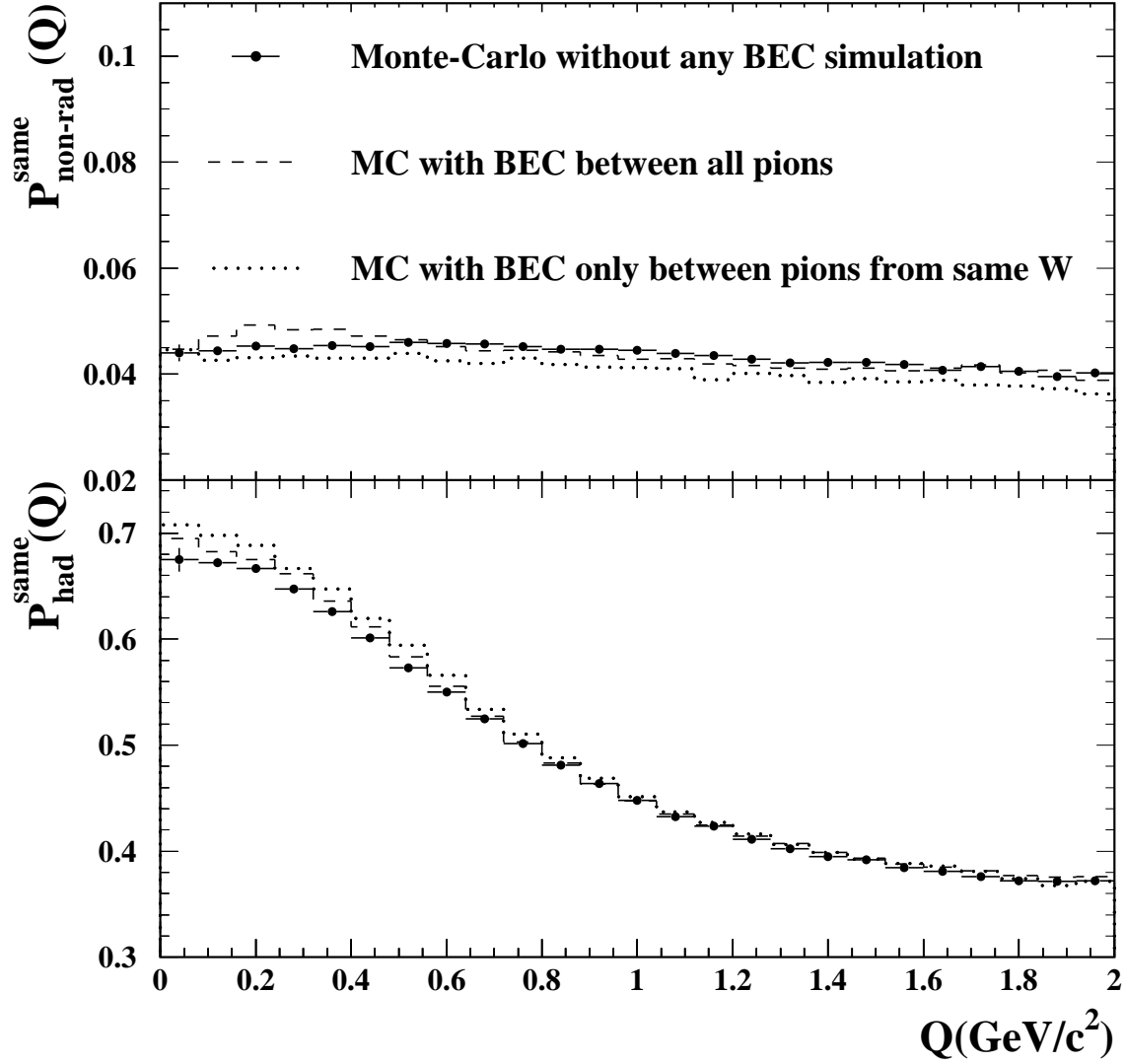


Figure 4: The probability that both tracks of an unlike-charge track pair in a fully hadronic event originate from the same W boson, $P_{\text{non-rad}}^{\text{same}}(Q)$ (upper plot) and $P_{\text{had}}^{\text{same}}(Q)$ (lower plot), as obtained from Monte Carlo simulations. The histogram is the result for the case that no BEC are assumed. The dashed and dotted histograms are the results for the case that BEC are simulated for all pions or only for pions originating from the same W boson, respectively.

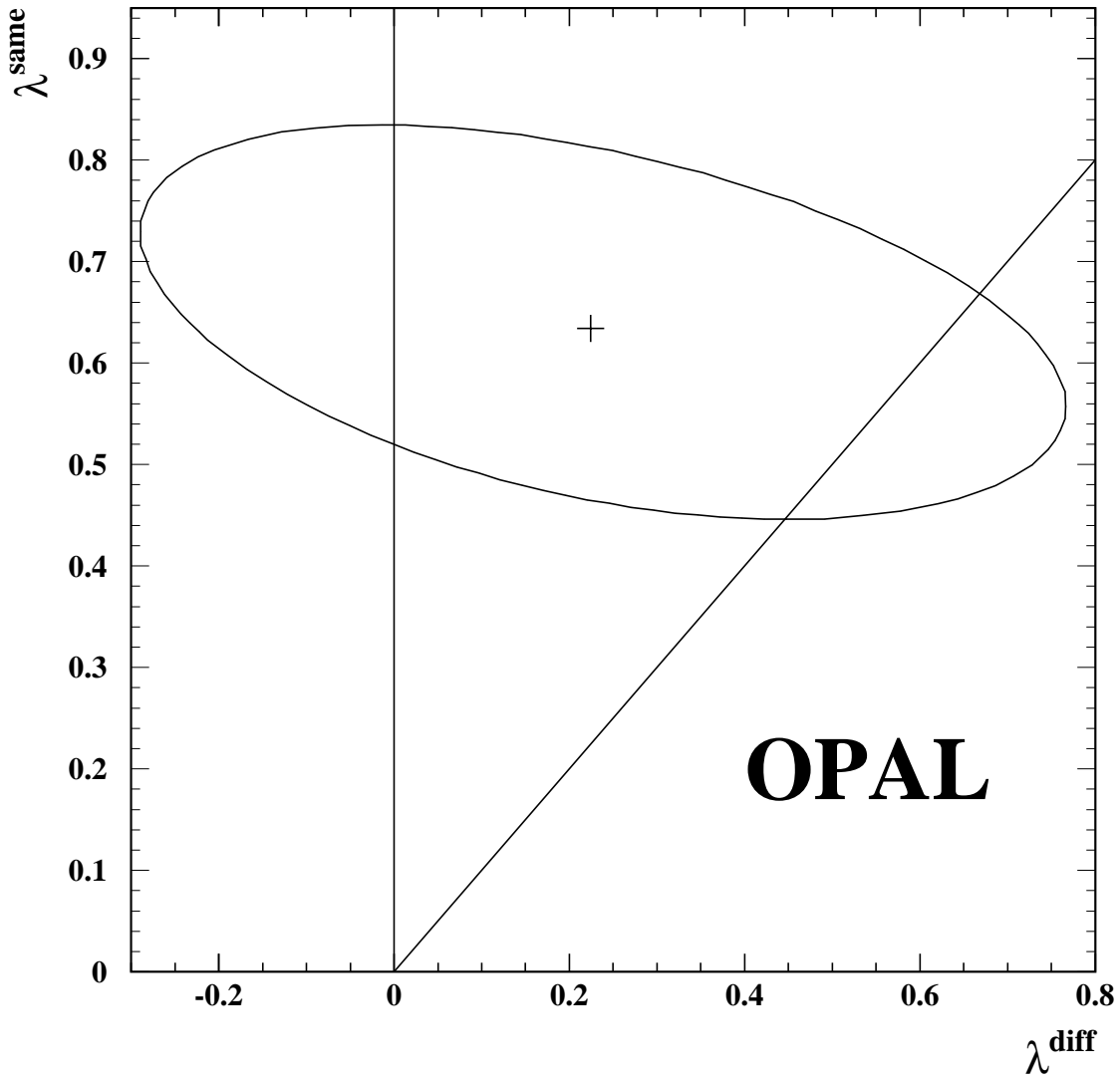


Figure 5: Correlation between λ^{diff} and λ^{same} . The contour shows the 67% confidence level. The best value obtained in the fit is given by the cross. The lines for $\lambda^{\text{diff}} = 0$ and $\lambda^{\text{diff}} = \lambda^{\text{same}}$ are also indicated.

3.3 Systematic Errors

The following variations in the analysis are considered to obtain the systematic error, which affect the fit result in both fit methods. The systematic errors are listed in Table 5 and 6, together with their quadratic sums to give the final systematic error.

1. *Variation of the resonance production.* In the main analysis, the distortion of the unlike-charge pairs due to resonances was taken into account by subtracting the resonance Q distribution from unlike-charge pair Q distribution. This method is based exclusively on Z^0 data, since no measurements of resonance production at LEP 2 are available. Thus for systematics the correction factors are varied within two standard deviations of the experimental resonance production cross sections. The maximum differences in the fit for each resonance were added in quadrature. Several variations were made for this systematic check, therefore no χ^2 is given. All fits are of good quality.
2. *Double-hit resolution.* Unlike-charge pairs are bent in a magnetic field in opposite directions, whereas like-charge pairs are bent in the same direction. Therefore like-charge pairs at very low Q are less well reconstructed. Monte Carlo studies indicate the presence of such effects for pairs with a Q less than $0.05 \text{ GeV}/c^2$. For systematics, the fit is repeated in the range between $0.05 < Q < 2.0 \text{ GeV}/c^2$.
3. *Use of the HERWIG Monte Carlo.* To determine the purities and the correction for resonances in the unlike-charge sample the HERWIG Monte Carlo was used.
4. The *probability functions* are obtained from Monte Carlo simulations where BEC are simulated [16] for all pions, both from the same and from different W bosons.
5. The *probability functions* are obtained from Monte Carlo simulations where BEC are simulated [16] only for pions from the same W.
6. *Long-range correlations.* The fit is repeated with $\epsilon = 0$.
7. *Different topology of the $(Z^0/\gamma)^* \rightarrow q\bar{q}$ background in fully hadronic selected events.* The difference of the $(Z^0/\gamma)^* \rightarrow q\bar{q}$ events in the hadronic and non-radiative Z^* samples is taken into account in the main analysis (see section 3.2). The events selected at LEP energies as $W^+W^- \rightarrow q\bar{q}q\bar{q}$ events and as non-radiative events, which are used for this correction are statistically limited. Therefore the parameters governing the correction factor for the correlation function $C_{\text{had}}^{Z^*}(Q)$ are varied within their statistical error ($\lambda \pm 0.04$ and $R \pm 0.057 \text{ fm}$) and the largest deviation is taken as the systematic error.

In addition, the effect on uncertainties from arising the knowledge of cross-section is examined. The cross-sections for W-pair production processes as well as the cross-section for non-radiative $(Z^0/\gamma)^*$ processes are varied within their experimental uncertainties. The impact on the final result is negligible. Furthermore, differences between $W^+W^- \rightarrow q\bar{q}q\bar{q}$ events selected as hadronic events and selected as non-radiative events are also considered. These variations introduce only small changes in the results.

	R (fm)	$\lambda^{W^+W^- \rightarrow q\bar{q}q\bar{q}}$	$\lambda^{W^+W^- \rightarrow q\bar{q}\ell\bar{\nu}_\ell}$	$\lambda^{(Z^0/\gamma)^* \rightarrow q\bar{q}}$	$\chi^2/\text{d.o.f.}$
Reference	0.91 ± 0.11	0.43 ± 0.15	0.75 ± 0.26	0.49 ± 0.11	76.1/62
Variation	δR (fm)	$\delta\lambda^{W^+W^- \rightarrow q\bar{q}q\bar{q}}$	$\delta\lambda^{W^+W^- \rightarrow q\bar{q}\ell\bar{\nu}_\ell}$	$\delta\lambda^{(Z^0/\gamma)^* \rightarrow q\bar{q}}$	
1	± 0.07	± 0.07	± 0.10	± 0.07	
2	< 0.01	-0.02	-0.05	$+0.03$	74.1/62
3	< 0.01	$+0.03$	$+0.05$	< 0.01	95.1/62
4	$+0.01$	-0.02	-0.02	-0.01	75.7/62
5	< 0.01	-0.02	-0.03	< 0.01	75.9/62
6	$+0.07$	-0.03	-0.13	-0.02	78.2/65
7	< 0.01	< 0.01	-0.01	< 0.01	76.3/62
total	0.10	0.09	0.18	0.08	

Table 5: The effect of the systematic variations studied (discussed in Sect. 3.3) on the variables R , $\lambda^{W^+W^- \rightarrow q\bar{q}q\bar{q}}$, $\lambda^{W^+W^- \rightarrow q\bar{q}\ell\bar{\nu}_\ell}$ and λ^{Z^*} . The last column shows the quality of the corresponding fit.

	R (fm)	λ^{same}	λ^{diff}	λ^{Z^*}	$\chi^2/\text{d.o.f.}$
Reference	0.92 ± 0.09	0.63 ± 0.19	0.22 ± 0.53	0.47 ± 0.11	76.4/64
Variation	δR (fm)	$\delta\lambda^{\text{same}}$	$\delta\lambda^{\text{diff}}$	$\delta\lambda^{Z^*}$	
1	± 0.07	± 0.09	± 0.07	± 0.07	
2	< 0.01	-0.05	< 0.01	$+0.03$	74.4/64
3	$+0.01$	$+0.04$	$+0.03$	< 0.01	94.5/64
4	$+0.01$	-0.02	-0.10	< 0.01	76.0/64
5	< 0.00	-0.04	-0.03	< 0.01	76.2/64
6	$+0.05$	-0.08	< 0.01	-0.01	77.6/66
7	< 0.01	< 0.01	-0.05	< 0.01	76.5/64
Total	0.09	0.14	0.14	0.08	

Table 6: The effect of the systematic variations studied (discussed in Sect. 3.3) on the variables R , λ^{same} , λ^{diff} and λ^{Z^*} . The last column shows the quality of the corresponding fit.

3.4 Q-based separation of BEC contributions

The experimental BEC for pure classes of a) tracks from different W bosons $C^{\text{diff}}(Q)$, b) tracks from the same W boson $C^{\text{same}}(Q)$, as well as c) tracks from $(Z^0/\gamma)^* \rightarrow q\bar{q}$ events $C^{Z^*}(Q)$ can be obtained directly from Eq. 12 - 14 by solving the equations for these three unknown functions for each bin of Q , using the fractions from Table 2. The resulting distributions are shown in Fig. 6. A comparison of data and Monte Carlo without BEC shows that there is a clear signal at small Q for pions originating from $(Z^0/\gamma)^* \rightarrow q\bar{q}$ events (Fig. 6 c). The data for pions from the same W boson show a larger enhancement than the corresponding simulation (Fig. 6 b). At the current level of precision, it cannot be established whether BEC between pions from different W bosons exists or not (Fig. 6 a), in agreement with the result of the simultaneous fit of Sect. 3.2. Note that the errors of the three unfolded distributions are highly correlated with each other *by construction*. For Q values larger than about $0.4 \text{ GeV}/c^2$, the distribution for $C^{\text{diff}}(Q)$ is consistent with being constant in both MC and data.

OPAL

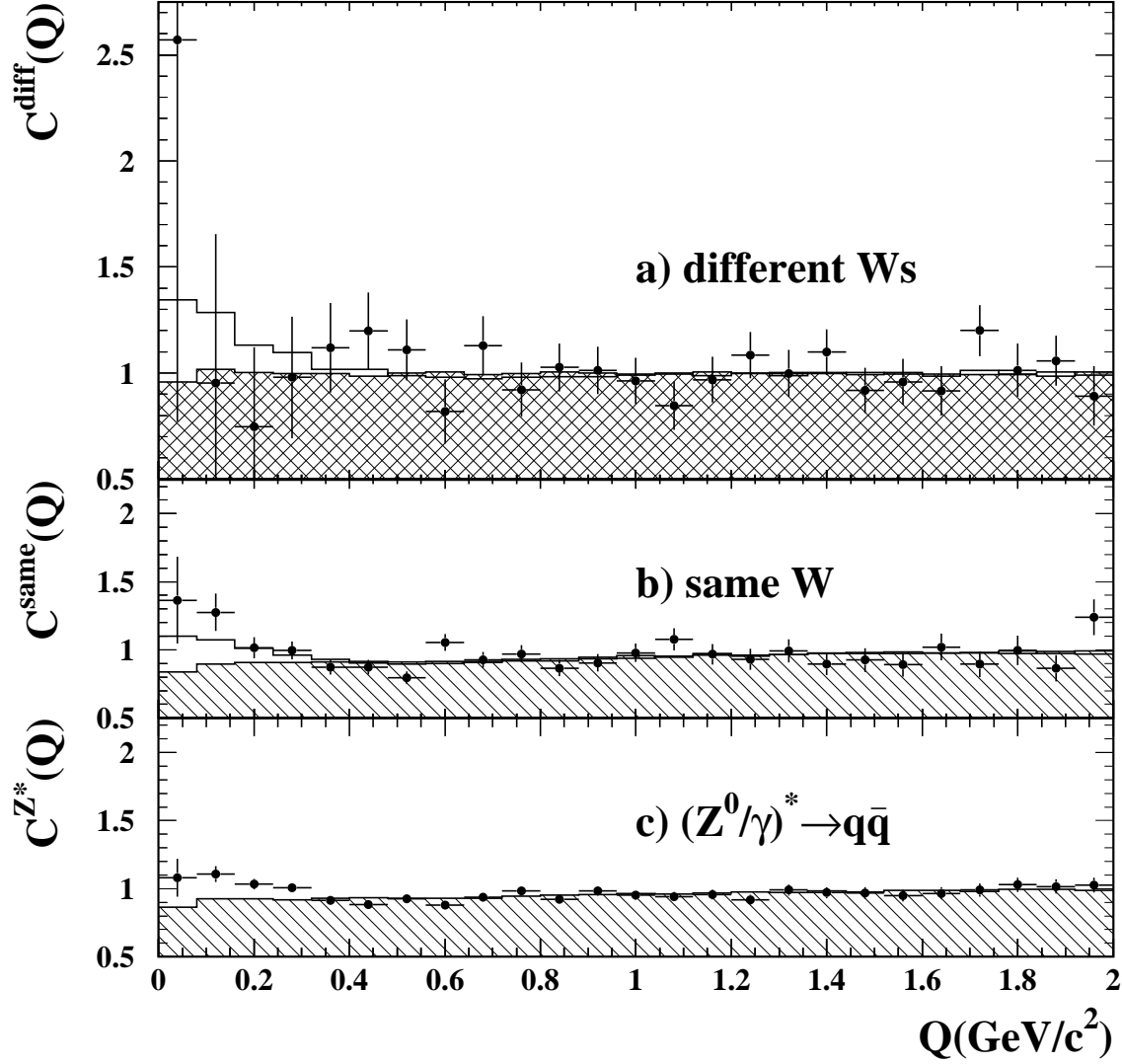


Figure 6: Correlation functions for the unfolded classes. The data points show the experimental distributions for a pure sample of a) pions originating from different W bosons $C^{\text{diff}}(Q)$, b) pions originating from the same W boson $C^{\text{same}}(Q)$ and c) pions from $(Z^0/\gamma)^* \rightarrow q\bar{q}$ events. The errors are the statistical uncertainties and are correlated between the three classes. The open histogram in a) is the result, for pions from different W bosons, of a simulation including BEC between pions from different W bosons, the cross-hatched histogram the corresponding result for a simulation with BEC for pions from the same W boson only. The open histogram in b) shows the result, for pions from the same W boson, of a simulation including BEC for pions from the same W boson and the hatched histogram the corresponding result for no BEC at all. The hatched histogram in c) corresponds to a simulation with no BEC at all.

3.5 Consistency check

In the analysis described above, the resonances were subtracted using Monte Carlo information and long-range correlations were taken into account by the empirical factor $(1 + \delta Q + \epsilon Q^2)$ in the correlation function of Eq. 4. As an alternative, we study here the double ratio

$$C'(Q) = \frac{N_{\pm\pm}^{DATA}}{N_{+-}^{DATA}} / \frac{N_{\pm\pm}^{MC}}{N_{+-}^{MC}}, \quad (15)$$

where the Monte Carlo events are generated without BEC. If the production of resonances⁴ and long-range correlations are well described by the simulation, these should cancel in the double ratio and only BEC should remain. The agreement between the simulation and data was checked and is good for both the unlike-charge and like-charge distributions. The latter show significant deviations only in the low Q region, where distortions due to BEC are expected in the data. Thus, for the double ratio, a simple fit ansatz can be used:

$$C'(Q) = N (1 + f_{\pi}(Q) \lambda e^{-Q^2 R^2}). \quad (16)$$

As in section 3.2, the double ratios for the three event selections can be described by superpositions of the correlations for the different pion classes. Eqs. 12 - 14 are also valid for the double ratios. It can be shown that the relative probabilities P are given by the expressions given in Table 2, except that, in this case, the number of like-charge pairs $N_{\pm\pm}$ have to be used instead of the number of unlike-charge ones N_{+-} as was the case in section 3.2. The relative probabilities are determined from a Monte Carlo simulation without BEC.

In a simultaneous fit to the three double ratios $C'(Q)$ the BEC for the three pion classes $C'^{\text{same}}(Q)$, $C'^{\text{diff}}(Q)$ and $C'^{Z^*}(Q)$ are determined. A common source radius for all pion classes is assumed and the parameters λ and R in the correlation function $C'^{Z^*}(Q)$ are adjusted for differences in multiplicity and topology as in section 3.2. The seven parameters used in the fit are given in Table 7. The fit is made in the full range $0.0 < Q < 2.0 \text{ GeV}/c^2$.

The fit describes the distributions well, with a $\chi^2/\text{d.o.f.}$ of 72.8/67. The results of the fit are given in Table 7. They are fully compatible with the results of section 3.2. The systematic errors are obtained in a similar way as before, with the relevant individual contributions given in Table 8. This method has the advantage that the long-range correlations do not have to be determined in the fit. On the other hand, this method relies more on Monte-Carlo input.

⁴As for the main analysis, the resonance cross-sections in JETSET are adjusted to the measured rates at LEP energies.

Parameter	same W	diff W	$(Z^0/\gamma)^*$
R (fm)		$1.11 \pm 0.13 \pm 0.21$	
λ	$0.65 \pm 0.21 \pm 0.09$	$0.50 \pm 0.78 \pm 0.14$	$0.42 \pm 0.09 \pm 0.05$
N	$0.99 \pm 0.01 \pm 0.03$	$1.00 \pm 0.01 \pm 0.00$	$0.99 \pm 0.01 \pm 0.02$

Table 7: Result of the simultaneous fit using the double ratio $C'(Q)$. The first error corresponds to the statistical uncertainty, the second one to systematics.

	R (fm)	λ^{same}	λ^{diff}	λ^{Z^*}	$\chi^2/\text{d.o.f.}$
Reference	1.10 ± 0.11	0.64 ± 0.20	0.50 ± 0.72	0.42 ± 0.09	72.8/68
Variation	δR (fm)	$\delta\lambda^{\text{same}}$	$\delta\lambda^{\text{diff}}$	$\delta\lambda^{Z^*}$	
1	± 0.11	± 0.07	± 0.03	± 0.09	
2	-0.14	-0.06	< 0.09	0.03	89.6/67
3	-0.12	< 0.01	$+0.06$	$+0.03$	91.5/67
7	< 0.01	< 0.01	$+0.01$	< 0.01	72.8/67
Total	0.21	0.09	0.14	0.05	

Table 8: The effect of the systematic variations studied (discussed in Sect. 3.3) on the variables R , λ^{same} , λ^{diff} and λ^{Z^*} from the double ratio. The last column shows the quality of the corresponding fit.

4 Discussion and Summary

We have analysed the data obtained by the OPAL detector at e^+e^- center-of-mass energies of 172 and 183 GeV to study BEC between pions in three different physical processes: fully hadronic events $W^+W^- \rightarrow q\bar{q}q\bar{q}$, semileptonic events $W^+W^- \rightarrow q\bar{q}\ell\bar{\nu}_\ell$, and non-radiative $(Z^0/\gamma)^*$ events. The analysis assumes equal source size R for these processes. BEC are observed each of these processes. The chaoticity parameter λ for the semileptonic process $W^+W^- \rightarrow q\bar{q}\ell\bar{\nu}_\ell$ is larger than for the processes $W^+W^- \rightarrow q\bar{q}q\bar{q}$ and $(Z^0/\gamma)^* \rightarrow q\bar{q}$, but still consistent within the errors. The long-range correlation parameters are consistent within their errors. Furthermore, BEC between pions from the same W boson and different W bosons have been studied. The result for pions from the same W boson is consistent with those for pions from non-radiative $(Z^0/\gamma)^* \rightarrow q\bar{q}$ events. At the current level of precision it is not established if BEC between pions from different W bosons exists or not.

5 Acknowledgements:

We particularly wish to thank the SL Division for the efficient operation of the LEP accelerator at all energies and for their continuing close cooperation with our experimental group. We thank our colleagues from CEA, DAPNIA/SPP, CE-Saclay for their efforts over the years on the time-of-flight and trigger systems which we continue to use. In addition to the support staff at our own institutions we are pleased to acknowledge the Department of Energy, USA,

National Science Foundation, USA,
Particle Physics and Astronomy Research Council, UK,
Natural Sciences and Engineering Research Council, Canada,
Israel Science Foundation, administered by the Israel Academy of Science and Humanities,
Minerva Gesellschaft,
Benozio Center for High Energy Physics,
Japanese Ministry of Education, Science and Culture (the Monbusho) and a grant under the Monbusho International Science Research Program,
Japanese Society for the Promotion of Science (JSPS),
German Israeli Bi-national Science Foundation (GIF),
Bundesministerium für Bildung, Wissenschaft, Forschung und Technologie, Germany,
National Research Council of Canada,
Research Corporation, USA,
Hungarian Foundation for Scientific Research, OTKA T-016660, T023793 and OTKA F-023259.

References

- [1] G. Goldhaber *et al.*, Phys. Rev. Lett. **3** (1959) 181; Phys. Rev. **120** (1960) 300.
- [2] W.A. Zajc in *Hadronic Multiparticle Production*, (Ed. P. Carruthers), World Scientific, 1988, p. 235;
S. Haywood, *Where are we going with Bose-Einstein - A mini review*, RAL Report 94-074.
E.A. De Wolf; *Bose-Einstein Correlations* in Proc. XXVII Int. Conf. on High Energy physics, Glasgow 20-27 July 1994 (Eds. P.J. Bussey and I.G. Knowles), Inst. of Physics Publ., 1995, p. 1281.
- [3] OPAL Collaboration, P.D. Acton *et al.*, Phys. Lett. **B267** (1991) 143.
- [4] OPAL Collaboration, G. Alexander *et al.*, Z. Phys. **C72** (1996) 389.
- [5] ALEPH Collaboration, D. Decamp *et al.*, Z. Phys. **C54** (1992) 75.
- [6] DELPHI Collaboration, P. Abreu *et al.*, Phys. Lett. **B286** (1992) 201.
- [7] OPAL Collaboration, P. Acton *et al.* Phys. Lett. **B298** (1993) 456.
- [8] OPAL Collaboration, R. Akers *et al.* Z. Phys. **C67** (1995) 389.
- [9] DELPHI Collaboration, P. Abreu *et al.* Phys. Lett. **B323** (1994) 242.
- [10] ALEPH Collaboration, D. Buskulic *et al.* Z. Phys. **C64** (1994) 361.
- [11] DELPHI Collaboration, P. Abreu *et al.*, Phys. Lett. **B379** (1996) 330.
- [12] L. Lönnblad and T. Sjöstrand, Phys. Lett., **B351** (1995) 293.

- [13] J. Häkkinen and M. Ringnér, Eur. Phys. J. **C5** (1998) 275.
- [14] V. Kartvelishvili, R. Kvatadze and R. Møller, Phys. Lett. **B408** (1997) 331.
- [15] S. Jadach and K. Zalewski, Acta. Phys. Polon. **B28** (1997) 1363.
- [16] L. Lönnblad and T. Sjöstrand, Eur. Phys. J. **C2** (1998) 165.
- [17] DELPHI Collaboration, P. Abreu *et al.*, Phys. Lett. **B401** (1997) 181.
- [18] OPAL Collab., K. Ahmet *et al.*, Nucl. Instrum. Methods **A305** (1991) 275;
S. Anderson *et al.*, Nucl. Inst. and Meth. **A403** (1998) 326.
- [19] O. Biebel *et al.*, Nucl. Instrum. Methods **A323** (1992) 169.
- [20] M. Hauschild *et al.*, Nucl. Instrum. Methods **314** (1992) 74.
- [21] OPAL Collaboration, K. Ackerstaff *et al.*, Eur. Phys. J. **C1** (1998) 395.
- [22] OPAL Collaboration, K. Ackerstaff *et al.*, W^+W^- production and triple gauge boson couplings at LEP, Submitted to Euro. Phys. J. C .
- [23] OPAL Collaboration, G. Alexander *et al.*, Phys. Lett. **B376** (1996) 232.
- [24] OPAL Collaboration, K. Ackerstaff *et al.*, Z. Phys. **C75** (1997) 193.
- [25] OPAL Collaboration, G. Alexander *et al.*, Z. Phys. **C52** (1991) 175.
- [26] M. Skrzypek *et al.*, Comp. Phys. Comm. **94**(1996) 216;
M. Skrzypek *et al.*, Phys. Lett. **372** (1996) 289.
- [27] T. Sjöstrand, Comp. Phys. Comm. **82** (1994) 74.
- [28] G. Marchesini *et al.*, Comp. Phys. Comm. **67** (1992) 465.
- [29] M. Gyulassy *et al.*, Phys. Rev. **C20** (1979) 2267.
- [30] T. Sjöstrand, Comp. Phys. Comm. **39** (1986) 347;
T. Sjöstrand and M. Bengtsson, Comp. Phys. Comm. **43** (1987) 367;
T. Sjöstrand, Comp. Phys. Comm. **82** (1994) 74.
- [31] I.G. Knowles and G.D. Lafferty, J. Phys. **G23** (1997) 731.